

# RSC Advances



This is an *Accepted Manuscript*, which has been through the Royal Society of Chemistry peer review process and has been accepted for publication.

*Accepted Manuscripts* are published online shortly after acceptance, before technical editing, formatting and proof reading. Using this free service, authors can make their results available to the community, in citable form, before we publish the edited article. This *Accepted Manuscript* will be replaced by the edited, formatted and paginated article as soon as this is available.

You can find more information about *Accepted Manuscripts* in the [Information for Authors](#).

Please note that technical editing may introduce minor changes to the text and/or graphics, which may alter content. The journal's standard [Terms & Conditions](#) and the [Ethical guidelines](#) still apply. In no event shall the Royal Society of Chemistry be held responsible for any errors or omissions in this *Accepted Manuscript* or any consequences arising from the use of any information it contains.

Cite this: DOI: 10.1039/c0xx00000x

www.rsc.org/xxxxxx

ARTICLE TYPE

## Acid base co-crystal converted into porous carbon material for energy storage devices

Inayat Ali Khan<sup>a</sup>, Amin Badshah<sup>a</sup>, Ataf Ali Altaf<sup>a</sup>, Nawaz Tahir<sup>b</sup>, Naghma Haider<sup>c</sup> and Muhammad Arif Nadeem<sup>\*a</sup>

Received (in XXX, XXX) XthXXXXXXXXXX 20XX, Accepted Xth XXXXXXXXXXXXX 20XX

DOI: 10.1039/b000000x

A simple and facile method is adopted for the synthesis of pure and catalyst free carbon material for supercapacitor applications. In co-crystal synthesis, the precursors (isophthalic acid and a base 4,4'-bipyridine) are arranged in regular pattern followed by carbonization at 600 °C under inert atmosphere to pure carbon material CIN-600. The obtained sample is characterized by many techniques like powder X-ray diffraction (PXRD), transmission electron microscopy (TEM), scanning electron microscopy (SEM), energy dispersive X-ray spectroscopy (EDS) and gas adsorption analysis. The gas adsorption and microscopic analysis have demonstrated the high porosity of the carbon sample with irregular geometry. Owing to the excellent porosity and electrical conducting properties, the CIN-600 has shown enhanced capacitive performance when used as electrode material in electric double layer capacitors. The specific capacitance of the sample is ca. 181.3 F g<sup>-1</sup> at 2 mV s<sup>-1</sup> and maintains 91.3% of its initial capacitance in long-term cycling test.

### Introduction

Co-crystals are solid materials under ambient conditions. Co-crystals comprise of two or more molecules known as co-crystal constructors. According to the Cambridge Structural Database (CSD) survey co-crystal represents less than 0.5% published crystal structures [1]. Co-crystals can be easily synthesized by invoking molecular structure, and the molecular interaction like the hydrogen bonding between the co-crystal formers. So far, co-crystal synthesis is limited to photopolymerization and nucleophilic substitution [2]. Their potential impact upon pharmaceutical formulation and green chemistry can never be ignored.

In the present study, for the first time, we have found the application of co-crystal in the synthesis of pure, catalyst free, cost effective and porous carbon material. The co-crystal (In-3) was synthesized from two co-formers; isophthalic acid (1,3-Benzenedicarboxylic acid) and 4,4'-bipyridine. The In-3 was structurally characterized by X-ray single crystal analysis and it was found that in In-3, the co-formers are arranged in polymeric chains via hydrogen bonding.

Supercapacitors or electric double layer capacitors (EDLCs) are modern electronic devices which work on the principle of double layer capacitance at the electrode/electrolyte interface where electric charges are accumulated on the electrode surfaces and ions of opposite charge are arranged at the electrolyte side. EDLCs are superior over modern secondary batteries because of their potential applications in high power output and high energy

density appliances. Supercapacitors are used in those electronic equipment's where tough power supply, high current drain is required and those that work under extreme environmental conditions [3]. The electrodes of supercapacitor consist of different carbon materials like carbon nanotubes (CNTs) [4], graphene [5], activated carbon [6], carbon onion [7], carbon fibers [8] and mesoporous carbon [9]. These carbon materials should be predominantly porous in nature to ensure proper accommodation of electrolyte ions. The surface area and porosity depends on the synthesis process and the nature of carbon precursor. Different sources like metal carbides [10–12], polymers [13], natural gas [14], natural silk [15], sucrose [16], furfuryl alcohol [17] and metal-organic frameworks (MOFs) [18–20] etc. have been used for the synthesis of carbon materials. Among the different methods, carbonization or template carbonization [21–28] is one of the synthetic route in which the carbon material could be obtained by heating the carbon source precursor at elevated temperatures. But this method suffers due to complex polymerization process at elevated temperature, selection of proper template which some time leads to the contamination of the final product, acid wash of the product to remove the metal/metal oxide derived from template or catalyst and low experimental yield. To address these limits there is a need of suitable carbon source and facile synthetic route.

In the present study, we are reporting a simple and facile method for the synthesis of carbon material via carbonization of solid-state co-crystal at 600 °C. To the best of our knowledge no report has been done so far where carbon material is derived from co-crystals. The co-crystal was synthesized under solvothermal

condition and characterized. The synthesized carbon material was checked as electrode material in supercapacitor.

## Experimental

### Synthesis of Co-crystal (In-3)

The In-3 was synthesized by mixing solutions of isophthalic acid (IPA) (1.0 mmol) and 4,4'-bipyridine (Bipy) (0.5 mmol) in 20% ethanol solution of water, stirred and introduced into a Teflon lined autoclave which was kept at 120 °C for 24 h followed by slow cooling to get yellow crystals. The product was filtered, washed with water and ethanol and dried under vacuum. Yield: 79%, Anal. Calcd.: C, 63.93% H, 4.13%, N, 5.74% Found: C, 63.84% H, 4.06% N, 5.61%. IR data ( $\nu_{\max}$  /  $\text{cm}^{-1}$ ): 3447 mbr, 3077 s, 1612 s, 1549 m, 1533 s, 1421 s, 1263 m, 1252 s, 1237 s, 1177 s, 1141 m, 1051 m, 1041 m, 976s, 968 m, 866.

### Pyrolysis of In-3

The In-3 (0.5 g) was grinded to fine powder and transferred into a ceramic boat which was placed in a quartz tube fixed in a tube furnace (Nabertherm B 180). Air was flushed away by continuous flow of Ar for 30 minutes. The sample was heated up to 600 °C (10 °C  $\text{min}^{-1}$ ) for 6 h under continuous flow of Ar gas and cooled slowly to room temperature. The carbon material (0.33 g) obtained was denoted as CIN-600 with total yield of 66%.

### Characterization

The single crystal X-rays diffraction data was collected on a Bruker kappa APEXII CCD diffractometer using graphite-monochromator Mo-K $\alpha$  radiation ( $\lambda = 0.71073 \text{ \AA}$ ) at ambient temperature. For data collection  $\omega$  scan and multi-scan absorption correction was applied. Final refinement on F2 was carried out by full-matrix least-squares techniques. Structure solution and refinements were accomplished with SHELXL-97 [29], WinGx [30], SAINT [31] and PLATON [32]. Wide angle X-ray diffraction measurements were carried out at a speed of 0.015  $\text{s}^{-1}$  by PANalytical diffractometer (X'Pert PRO 3040/60) with a Cu K $\alpha$  ( $\lambda = 1.544206 \text{ \AA}$ ) radiation generated at 40 kV and 30 mA. Surface morphology of CIN-600 was examined by scanning electron microscope (JEOL-JSM-6610LV) equipped with energy dispersive X-ray spectroscopy (EDS). TEM analysis of the sample was conducted with FEI Company's Titan 80-300 CT transmission electron microscope with the acceleration voltage of 300 kV.  $\text{N}_2$  adsorption/desorption measurements were carried out using the Accelerated Surface Area & Porosity System 2020 supplied by Micromeritics Instruments Inc. Approximately 20 mg of sample was loaded into a glass analysis tube and outgassed for 3 h under vacuum at 200 °C prior to measurement. The isotherm was measured at 77 K and data was analyzed using Bruner-Emmett-Teller (BET) model to determine the surface area. The pore size distribution plot was conducted on the adsorption branch of the isotherm based on density functional theory (DFT) model. FT-IR analysis was carried out on a Thermoscientific NICOLET 6700 FTIR.

### Electrochemical studies

For electrode preparation, a black slurry was prepared by mixing 5 mg of CIN-600 with 5 mL ethanol and 10  $\mu\text{L}$  Nafion (5 wt.%) solution which was sonicated for 30 minutes. After evaporating

ethanol, the black slurry was pressed between two pieces of nickel foam (1 cm  $\times$  1 cm) under 350  $\text{kg cm}^{-2}$  (using hydraulic presser EQ-HP-88V220). After drying at 100 °C the electrode was impregnated with electrolyte solution overnight to ensure complete saturation of the electrode materials with electrolyte ions. The designed electrode was subjected for electrochemical studies in a three electrode cell assembly using 6 mol  $\text{L}^{-1}$  KOH. The cell assembly consists of CIN-600 sample electrode as the working, platinum wire as the auxiliary and Ag/AgCl as the reference electrode. All the electrochemical measurements were carried out by Biologic SP 300 electrochemical analyzer at room temperature.

## Results and Discussions

### Characterization

The single crystal X-ray structural analysis of In-3 is presented in Figure 1 and the crystallographic data and structure refinement parameters are tabulated in Table S1 (supplementary information). The crystallographic data has been deposited in the CCDC and can be obtained free of charge from The Cambridge Crystallographic Data Centre via [www.ccdc.cam.ac.uk/data\\_request/cif](http://www.ccdc.cam.ac.uk/data_request/cif) quoting: CCDC 1002755.

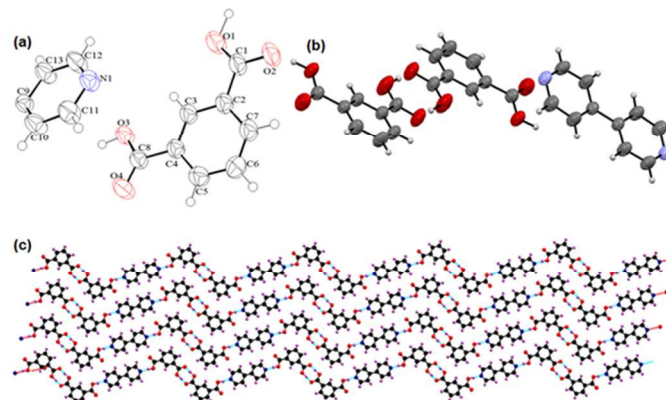


**Figure 1.** (a) Asymmetric unit of co-crystal In-3, (b) molecular structure of the In-3 that consists of two acids and one base molecule, (c) 2D sheet of In-3 formed by the inter-tape CH --- O type hydrogen bonding, the zig zag tape structure of In-3 formed by the intermolecular OH --- O and OH --- N type hydrogen bonding.

The crystal structure reveals that In-3 formed by the coupling of IPA and Bipy in 2:1 ratio [Figure 1 (b)]. In In-3, two IPA molecules coupled by OH---O type hydrogen bonding and formed a six member planer ring and this pair form OH---N type hydrogen bond with Bipy which leads to a zigzag tape structure. CH---O type hydrogen bonding assemble these zigzag tapes into a sheet structure [Figure 1 (c)]. Similar type of co-crystal structure has been reported by Shan et al. [33, 34]. The layer by layer packing of 2D sheets in the crystal packing motivates us to carbonize the co-crystal in order to get ordered carbon material. The PXRD pattern of CIN-600 revealed the formation of pure carbon material. The heteroatoms like N and O in the In-3 were converted into  $\text{NO}_x$ ,  $\text{O}_2$  and  $\text{CO}_x$  and vaporized in Ar flow environment. Broad peaks at  $2\theta = 25^\circ$  and  $2\theta = 45^\circ$  in the XRD pattern of CIN-600 [Figure 2] corresponds to the (002) and (100)

crystallographic planes of carbon material. To evaluate the degree of graphitization, the empirical parameter ( $R$ ) was used, which can be defined as the ratio of the height of the (002) Bragg peak to the background [25, 26].  $R$  factor for CIN-600 sample is 0.62 which shows that some graphitic sheets are also present along with other types of carbon matrix.

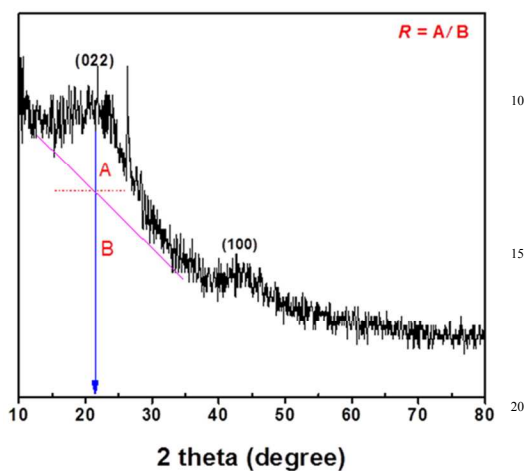


Figure 2. Powder XRD pattern of CIN-600.

To evaluate the surface area and the pore size distribution  $N_2$  adsorption/desorption analysis were performed and the isotherm is shown in Figure 3. Type-IV isotherm is found for CIN-600 sample suggesting the existence of different pore sizes ranging from micro to mesopores. At high relative pressure hysteresis between adsorption and desorption branches demonstrates the presence of mesopores in the surface texture. The BET surface area of CIN-600 sample is  $1230\text{m}^2\text{g}^{-1}$  with pore diameter of 2.13 nm.

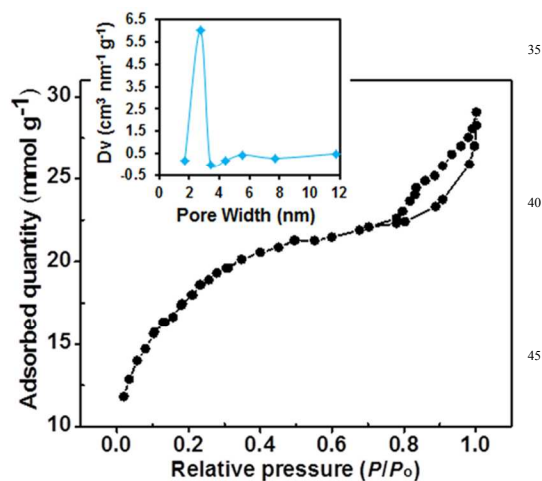


Figure 3.  $N_2$  adsorption/desorption isotherm and pore size distribution (inset) of CIN-600 carbon sample.

To characterize the surface morphology of the sample, TEM and SEM analysis was conducted and the obtained images are presented in Figure 4. TEM images [Figure 4 (a, b)] shows micro-porous nature of amorphous carbon. It is obvious that the surface texture of samples is porous with monolithic irregular shape. The SEM images of CIN-600 sample [Figure 4 (c, d)]

show clear and well define pores created at the surface during fabrication of CIN-600 carbon sample. These pores and ruptured surface is developed by the exclusion of gases like  $\text{CO}_x$ ,  $\text{NO}_x$  during carbonization under Ar atmosphere. The porosity of the carbon material has a very important role in the capacitance of a capacitor. Carbon material with proper pore size and distribution is required to show good capacitive performance. The pores of carbon material can facilitate the inside diffusion of ions during charge-discharge operating conditions. Here in the present study, the CIN-600 sample has exhibited good capacitive performance due to the porous nature as clear from gas adsorption and microscopic analysis. EDX analysis was carried out to confirm the percent composition and purity of CIN-600 sample. The FT-IR analysis also support the purity of carbon material (Figure S1). EDX spectrum has [Figure 4 (e)] a single point at ca. 0.25 keV for carbon which suggests the high purity of the obtained sample.

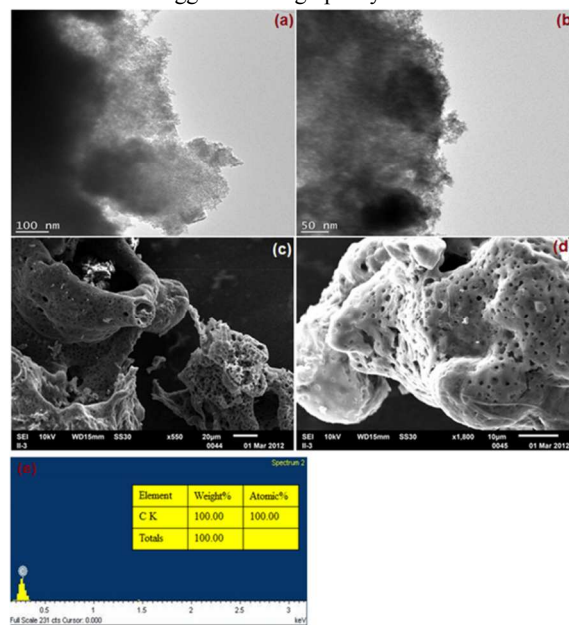


Figure 4. TEM micrographs (a, b), SEM images (c, d) and EDX spectrum of CIN-600 (e).

### Electrochemical Evaluation

The working principle of supercapacitor is the accumulation of electrolyte ions in the electric double layer developed by the electrostatic force. The capacitance (energy stored by electrode) largely depends on the surface interaction of electrode and electrolyte. There is direct relationship between specific capacitance and surface area:  $C_{sp} = \epsilon S/d$ ; ( $C_{sp}$  = specific capacitance,  $\epsilon$  = permittivity of electrolyte,  $S$  = surface area of the electrode-electrolyte interface,  $d$  = distance between the polarized carbon surface and maximum charge density of solvated ions) [27, 28]. However, the surface which can be electrochemically accessed by the solvated ions only makes contribution to the capacitance. The pore size of the electrode materials should be properly matched with the size of the solvated ions for excellent capacitive performance. In addition, the capacitance of a capacitor also depends on surface wettability, applied pressure for packing and electrical conductivity of the electrode materials.

The voltammograms of the CIN-600 sample are presented in Figure 5 (a) with different voltage scan rates from 2  $\text{mV s}^{-1}$  to 150  $\text{mV s}^{-1}$  in the potential range of  $-0.1 \text{ V}$  to  $+0.5 \text{ V}$ . The sample has excellent capacitive behavior as obvious from the fairly rectangular shape of voltammograms in the given range of potential scan rates. The box like rectangular shape of voltammograms with increasing voltage sweep rate suggests that the electrode material is quite suitable for quick charge-discharge operation condition. Generally, better capacitive behavior of a sample at high voltage sweep rate is attributed to the better accessibility of ions to the electrochemically active surface area. It is believed that the capacitive performance of the carbon materials depends on the pore size which favors the penetration of solvated ions. The excellent capacitive performance of CIN-600 sample can also be attributed to its large porosity as presented in gas adsorption and microscopic studies. The specific capacitance ( $\text{F g}^{-1}$ ) from CV curves were calculated using the following equation;  $C_{\text{sp}} = (\Delta Q)/(\Delta V \times m)$  where ' $\Delta Q$ ' is the charge (C) integrated from the whole voltage range, ' $\Delta V$ ' is the whole voltage (V) difference, and ' $m$ ' is the mass (g) of carbon on the electrode. The calculated values of specific capacitance are given in Table S2 (supplementary information) for CIN-600 sample. As can be seen in the data that the sample CIN-600 have the highest capacitance of  $181.3 \text{ F g}^{-1}$  at sweep rate of  $2 \text{ mV s}^{-1}$  and lowest capacitance value of  $122.3 \text{ F g}^{-1}$  at voltage sweep rate of  $150 \text{ mV s}^{-1}$ . At low sweep rate the ions have sufficient time to diffuse into the pores of sample while at high voltage scan rate the ions can only penetrate into some external large pores with fast movement.

The relationship between the ratio of retained capacitance and voltage scan rate is plotted and presented in Figure 5 (c). There is a decrease in the ratio of retained capacitance with increase in voltage scan rate, showing the limited use of electrochemically active surface area at high scan rate in comparison to low scan rate. However, the sample retains about 66% of its initial capacitance even at high scan rate of  $150 \text{ mV s}^{-1}$ .

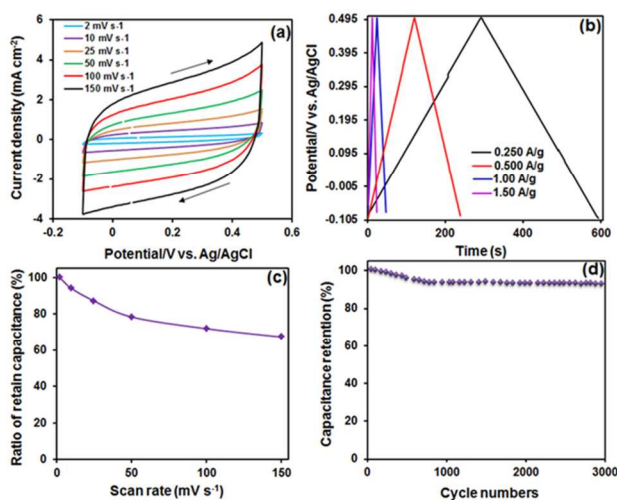


**Figure 5.** Cyclic voltammetric curves from 2 to  $150 \text{ mV s}^{-1}$  potential sweep rates (a), galvanostatic charge/discharge curves at different current densities (b), plot of retain capacitance versus scan rates (c), and long-term cycling (d) of CIN-600 sample.

Galvanostatic charge/discharge tests were also carried out in the potential window of  $-0.1 \text{ V}$  to  $+0.5 \text{ V}$  at different current density from  $0.250$  to  $1.5 \text{ A g}^{-1}$  to evaluate the capacitive performance of the carbon material and the results are shown in Figure 5(b). Specific capacitance was calculated by the equation;  $C_{\text{sp}} = (I \times \Delta t)/(\Delta V \times m)$ , where ' $I$ ' is the constant discharge current, ' $\Delta t$ ' is the discharge time, ' $\Delta V$ ' is the voltage difference, and ' $m$ ' is the mass of the carbon material. The specific capacitance from charge/discharge measurements at different current densities are given in Table S2. It is clear that the charging curve is almost symmetrical with their corresponding discharge counterpart and the linear voltage-time relationship with no obvious voltage drop indicates good capacitive behavior of the CIN-600 carbon sample. The galvanostatic charge/discharge results are well consistent with voltammetric measurements illustrating an ideal capacitor behavior. Cycling charge/discharge measurements were conducted at  $0.500 \text{ A g}^{-1}$  to test the long-term cycling stability of the carbon electrode material [Figure 5 (d)]. The CIN-600 sample maintains almost 91.3% of their initial capacitance after 3000 cycles presenting its good long-term cyclic stability. Figure 6 shows that voltammetric currents are almost proportional to the scan rate of CV. The slope of  $i-v$  lines is dependent upon the measured potential. The linear dependency of current on scan rates of CV illustrates the high-power characteristics of the CIN-600 sample.

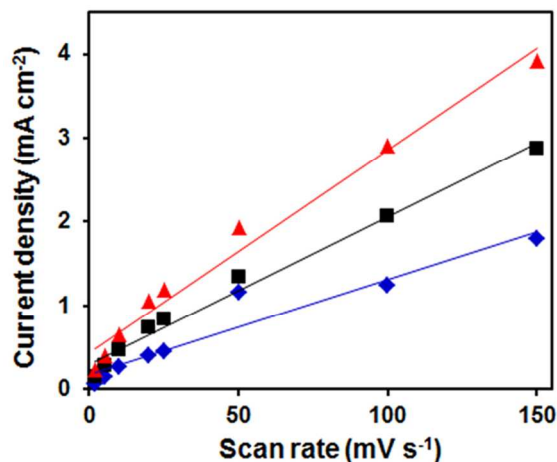


**Figure 6.** Plot of current density versus potential scans rates ( $i-v$ ) from CV results where the current was obtained at:  $0.0 \text{ V}$ ,  $0.2 \text{ V}$ , and  $-0.4 \text{ V}$ .

The electrochemical performance of CIN-600 is comparable with most of the recently reported porous carbon materials synthesized by complicated and tedious process. A few reports are described here for reference. Lu *et al.*, have obtained ordered mesoporous carbon (OMCs) from sucrose with controllable pore sizes in the range of  $4-10 \text{ nm}$  by a template procedure using 2D hexagonal MSU-H and 3D cubic KIT-6 silica as hard templates and boric acid as the pore expanding agent. The prepared OMCs have exhibited the specific capacitance values from  $143$  to  $205 \text{ F g}^{-1}$  at  $5 \text{ mV s}^{-1}$  [38]. Li *et al.*, synthesized nitrogen enriched microporous carbon spheres (MCS) by the polymerization-induced colloid aggregation method with BET area of ca.  $1330 \text{ m}^2 \text{ g}^{-1}$ . As electrode material for electric double layer capacitors the MCS have shown specific

capacitance value of up to 211 F g<sup>-1</sup> at a discharge current density of 1 A g<sup>-1</sup> [39]. Song and coworkers have prepared phenolic based carbon nanofiberswebs (PCNFWs) by electrospinning resole-type phenolic resin/PVA blend solution, followed by curing and carbonization [40]. The specific surface area of the carbon was 416 m<sup>2</sup> g<sup>-1</sup> and the specific capacitance value of up to 171 F g<sup>-1</sup> at 5 mV s<sup>-1</sup>. Jin and coworkers [41] have reported novel carbon-based microporous nanoplates containing numerous heteroatoms (H-CMNs) from regenerated silk fibroin. The BET surface area of the carbon product was 2557.3 m<sup>2</sup> g<sup>-1</sup> similar to pristine graphene sheet. The H-CMNs have exhibited specific capacitance up to 264 F g<sup>-1</sup> at 0.1 A g<sup>-1</sup> current density in 1 mol L<sup>-1</sup> H<sub>2</sub>SO<sub>4</sub>. Guo *et al.*, [42] have prepared microporous carbon materials by carbonization of sulfuric acid pretreated sucrose. The pore size and BET surface area were in the ranges of 0.7–1.2 nm and 178–603 m<sup>2</sup> g<sup>-1</sup> respectively. It was concluded that the sample carbonized at 800 °C displayed the highest surface area and highest specific capacitance up to 232 F g<sup>-1</sup> at 0.1 A g<sup>-1</sup> current density. Xu and coworkers [43] used metal-organic framework (MOF) as a template and furfuryl alcohol as a precursor for the synthesis of nanoporous carbon (NPCs). The BET surface area of the NPCs fall in the range of 1140 to 3040 m<sup>2</sup> g<sup>-1</sup> and the pore size distribution centered at about 3.9 nm. They have concluded that the NPCs samples obtained at a temperature higher than 600 °C have almost constant specific capacitance up to 100 F g<sup>-1</sup> at 5 mV s<sup>-1</sup> while the NPC sample obtained at 530 °C gives rise to specific surface area of 3040 m<sup>2</sup> g<sup>-1</sup> but lowest specific capacitance of 12 F g<sup>-1</sup> at 5 mV s<sup>-1</sup>.

The electrochemical behavior of carbon sample CIN-600 was further evaluated by impedance spectroscopy. Generally the Nyquist spectrum is divided into high frequency semicircle region attributed to the charge transfer resistance occurring at the electrode/electrolyte interface and the low frequency curve with 45° slope representing the Warburg diffusion resistance [35]. The impedance study of CIN-600 carbon electrode in 6 mol L<sup>-1</sup> KOH solution in the frequency range of 1 to 100,000 Hz (at 10 mV as potential amplitude) is shown in Figure 7. The Nyquist plot [Figure 7 (a)] consists of two parts, the horizontal line (with real axis) at high frequency region and the 45° slope at low frequency region. The absence of the semicircle in the spectrum suggests very good ionic conductivity at the electrode/electrolyte interface [36, 37]. Between the horizontal line and the 45° slope, there is a transition zone (at resistance of 2.3 Ω) which is believed to be due to the ionic mobility in the pores of carbon, which affect the capacitive performance of the electrode at high current drain [25]. The 45° slope at low frequency region indicates an ideal capacitive behavior of the carbon material. This further demonstrates that the carbon material can store significant value of electrical energy at low frequency in the electric double layer. The frequency response (FR) of the electrode material has been depicted from the impedance measurement and the plot is presented in Figure 7 (b). The FR reflects the number of solvated ions reached at the porous surface at a specific frequency of alternating current. It is clear from Figure 7 (b) that the imaginary part of impedance (capacitive part) decreases with increase in frequency presenting a drop in capacitance which is quite significant at value higher than 10 Hz. The overall map of the FR study demonstrates a better capacitive performance of the

electrode materials which may be due to the proper combination of micro and meso-pores in which the former will favor a better efficiency of ionic access to the electrochemically active surfaces at low frequencies while the later will facilitate ionic diffusion at high frequencies.

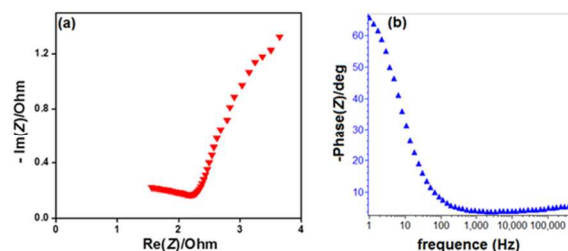


**Figure 7.** The electrochemical impedance spectrum (a), Bode angle plot from impedance measurements (b) of CIN-600.

## Conclusions

Porous carbon material was obtained by the simple carbonization of rigid co-crystal using the self-degradation template method. The carbonization was carried out at 600 °C in an argon atmosphere for 6 h in order to obtain pure carbon product. During gas adsorption and SEM analysis it was found that the sample CIN-600 is very porous. Due to the porous nature the sample was subjected as electrode material in EDLCs. In CV studies the sample has exhibited good voltammetric behaviour with specific capacitance of 181.3 F g<sup>-1</sup> at 2 mV s<sup>-1</sup> and 122.3 F g<sup>-1</sup> at 150 mV s<sup>-1</sup>. The good frequency response during electrochemical impedance measurement further confirms the excellent capacitive candidature of the sample. Given the broad range of acids and basis, a great variety of co-crystals with different dimensionality and porosity can be synthesized and converted into broad range of carbon materials which can also be structurally tuned via judicious choice of co-formers. These preliminary results open up a new research gateway towards synthesis of multifunctional carbon materials.

## Acknowledgments

The work was financially supported by Higher Education Commission (HEC) of Pakistan (PD-IPFP/HRD/HEC/2013/1933 and 20-1638/R&D/09/2900).

Notes and references

- <sup>a</sup>*Catalysis and Nanomaterials Lab 27 Department of Chemistry Quaid-i-Azam University, Islamabad 45320, Pakistan, Tel: +92-51-90642062; E-mail: arifchemist@hotmail.com*
- <sup>b</sup>*Department of Physics University of Sargodha, Sargodha 40100, Pakistan*
- <sup>c</sup>*Geoscience Advanced Research Laboratories, Geological Survey of Pakistan, Chakshahzad Town, Islamabad, Pakistan.*
- [1] M. L. Cheney, G. J. McManus, J. A. Perman, Z. Wang and M. J. Zaworotko, *Cryst Growth Des*, 2007, **7**, 616–617.
- [2] M. C. Etter, G. M. Frankenbach and J. Bernstein, *Tetrahedron*, 1989, **30**, 3617–3620
- [3] A. Chu and P. Braatz, *J Power Sources*, 2002, **112**, 236–246
- [4] L. B. Hu, J. W. Choi, Y. Yang, S. Jeong, F. LaMantia, L. F. Cui and Y. Cui, *Proc Natl Acad Sci, USA*, 2009, **106**, 21490–21494
- [5] H. M. Jeong, J. W. Lee, W. H. Shin, Y. J. Choi, H. J. Shin, J. K. Kang and J. W. Choi, *NanoLett*, 2011, **11**, 2472–2477
- [6] A. G. Pandolfo and A. F. Hollenkamp, *J Power Sources*, 2006, **157**, 11–27

- [7] D. Pech, M. Brunet, H. Durou, P. Huang, V. Mochalin, Y. Gogotsi, P. L. Taberna and P. Simon, *Nat.Nanotechnol.*, 2010, **5**, 651–654.
- [8] E. Frackowiak and F. Béguin, *Carbon*, 2001, **39**, 937–950.
- [9] S. R. S. Prabaharan, R. Vimala and Z. Zainal, *J. Power Sources*, 2006, **161**, 730–736.
- [10] M. Arulepp, J. Leis, M. Latt, F. Miller, K. Rummaa, E. Lust and A. F. Burke, *J. Power Sources*, 2006, **162**, 1460–1466.
- [11] Y. Gogotsi, A. Nikitin, H. Ye, W. Zhou, J. E. Fischer, B. Yi, H. C. Foley and M. W. Barsoum, *Nat. Mater.*, 2003, **2**, 591–594.
- [12] A. Jänes, T. Thomberg and E. Lust, *Carbon*, 2007, **45**, 2717–2722.
- [13] J. Sutasinpromprae, S. Jitjaicham, M. Nithitanakul, C. Meechaisue and P. Supaphol, *Polym. Int.*, 2006, **55**, 825–833.
- [14] J. Kong, A. M. Cassell and H. Dai, *ChemPhysLett*, 1998, **292**, 567–574.
- [15] Y. Liang, D. Wu and R. Fu, *Sci Rep.*, 2013, **3**, 1–5.
- [16] J-K. Kim, G. Cheruvally and J-H. Ahn, *J. Solid State Electrochem.* 2008, **12**, 799–805.
- [17] T. Kyotani, L. Tsai and A. Tomita, *Chem Mater.*, 1996, **8**, 2109–2113.
- [18] B. Liu, H. Shioyama, T. Akita and Q. Xu, *J. Am. Chem. Soc.*, 2008, **130**, 5390–5391.
- [19] S. J. Yang, T. Kim, J. Hyuklm, Y. S. Kim, K. Lee, H. Jung and C. R. Park, *Chem Mater*, 2012, **24**, 464–470.
- [20] I. A. Khan, A. Badshah, N. Haider, S. Ullah, D. H. Anjum and M. A. Nadeem, *J. Solid State Electrochem*, 2014, **18**, 1545–1555.
- [21] C. Journet, W. K. Maser, P. Berier, A. Loiseau, M. L. Chapelle, S. Lefrant, P. Deniard, R. Lee and J. E. Fischer, *Nature*, 1997, **388**, 756–758.
- [22] A. Thess, R. Lee, P. Nikolaev, H. Dai, P. Peti, J. Robert, C. Xu, Y. H. Lee, S. G. Kim, A. G. Rinzler, D. T. Colbert, G. E. Scuseria, D. Tománek, J. E. Fischer and R. E. Smalley, *Science*, 1996, **273**, 483–487.
- [23] B. Zheng, C. Lu, G. Gu, A. Makarovski, G. Finkelstein G and J. Liu, *NanoLett*, 2002, **2**, 895–898.
- [24] A. Ahmadpour and D. D. Do, *Carbon*, 1996, **34**, 471–479.
- [25] J. Hu, H. Wang, Q. Gao and H. Guo, *Carbon*, 2010, **48**, 3599–3606.
- [26] K. S. Park, Z. Ni, A. P. Cote, J. Y. Choi, R. Huang, F. J. Uribe-Romo, H. K. Chae, M. O’Keeffe and O. M. Yaghi, *Pro Natl Acad Sci U S A*, 2006, **103**, 10186–10189.
- [27] D. Lozano-Castello, D. Cazorla-Amoros, A. Linares-Solano, S. Shiraishi, H. Kurihara and A. Oya, *Carbon*, 2004, **41**, 1765–1775.
- [28] H. Shi, *ElectrochimActa*, 1996, **41**, 1633–1639.
- [29] G. M. Sheldrick, *Acta Crystallogr Sect A*, 2008, **64**, 112–122.
- [30] L. J. Farrugia, *J. Appl Crystallogr*, 1999, **32**, 837–838.
- [31] Bruker APEX2 and SAINT Bruker AXS Inc., Madison, Wisconsin, USA (2007).
- [32] A. L. Spek, *Acta Crystallogr Sect D*, 2007, **65**, 148–155.
- [33] N. Shan, A. D. Bond and W. Jones, *Cryst Eng*, 2002, **5**, 9–24.
- [34] C. Meiners, S. E. Valiyaveetil and V. Mullen, *J. Mater Chem*, 1997, **7**, 2367–2374.
- [35] W. Sugimoto, K. Yokoshima, Y. Murakami and Y. Takasu, *Electrochim Acta*, 2006, **52**, 1742–1748.
- [36] J. Chmiola, G. Yushin, Y. Gogotsi, C. Portet, P. Simon and P. L. Taberna, *Science*, 2006, **313**, 1760–1763.
- [37] R. Lin, P. Taberna, L. Chmiola, D. Guay, Y. Gogotsi and P. Simon, *J. Electrochem Soc.*, 2009, **156**, A7–A12.
- [38] H. Lu, W. Dai, M. Zheng, N. Li, G. Ji and J. Cao, *J. Power Sources*, 2012, **209**, 243–250.
- [39] W. Li, D. Chen, Z. Li, Y. Shi, Y. Wan, J. Huang, J. Yang, D. Zhao and Z. Jiang, *Electrochem. Commun.* 2007, **9**, 569–573.
- [40] C. Ma, Y. Song, J. Shi, D. Zhang, M. Zhong, Q. Guo and L. Liu, *Mater. Lett.* 2012, **76**, 211–214.
- [41] Y. S. Yun, S. Y. Cho, J. Shim, B. H. Kim, S.-J. Chang, S. J. Baek, Y. S. Huh, Y. Tak, Y. W. Park, S. Park and H.-J. Jin, *Adv. Mater.* 2013, **25**, 1993–1998.
- [42] P. Guo, Y. Gu, Z. Lei, Y. Cui and X. S. Zhao, *Microporous Mesoporous Mater.* 2012, **156**, 176–180.
- [43] B. Liu, H. Shioyama, H. Jiang, X. Zhang and Q. Xu, *Carbon*, 2010, **48**, 456–463.